AIAA JOURNAL
Vol. 41, No. 4, April 2003

Throat Heating Effect on Critical Roughness and Nozzle Wall Boundary-Layer Stability

R.-S. Lin,* V. Iyer,† and M. R. Malik‡
High Technology Corporation, Hampton, Virginia 23666

The effect of wall heating in the throat region on the flow quality in a Mach 3.5 and a Mach 2.4 axisymmetric nozzle is investigated. Because of the boundary-layer thickening effect, the critical roughness height to trigger laminar–turbulent transition is larger in the heated cases. Therefore, for a given surface finish, the adverse effect of roughness on transition can be minimized by sufficient wall heating. However, the combined effect of heating and pressure gradients is to introduce an overshoot in the streamwise velocity profile, as earlier predicted by Cohen and Reshotko. Associated with this overshoot is a new generalized inflection point near the edge of the boundary layer, and, as a consequence, the nozzle wall boundary layer supports high-frequency two-dimensional inviscid disturbances. *N*-factor results indicate that, with excessive throat heating, these disturbances could cause premature transition downstream of the throat and, hence, jeopardize the quiet performance. Therefore, favorable (on critical roughness height) and adverse (on boundary-layer instability) effects of heating have to be carefully evaluated. Mean flows are computed by using both a boundary-layer code and a Navier–Stokes solver, the critical roughness heights are calculated based on an empirical formula, and the destabilizing effect of heating is evaluated by using compressible linear stability theory. The critical roughness heights are established for the two nozzles for given heating strips.

I. Introduction

A QUIET supersonic nozzle is one in which an extended run of laminar flow is maintained in the nozzle wall boundary layer yielding a low-disturbance freestream in the wind-tunnel test section. Laminar–turbulent transition in the nozzle wall boundary layer limits the extent of this low-disturbance test section. Because transition location on a model placed in the test section is adversely affected by high noise, quiet supersonic facilities are required for simulating the flight environment.

The performance of a quiet nozzle can be characterized by the magnitude of a Reynolds number $Re_{\Delta x}$, which is based on the freestream conditions and the length of the quiet test core Δx. Figure 1 (from Ref. 1) shows $Re_{\Delta x}$ from test data for two NASA Langley Research Center rapid-expansion (RE) pilot quiet nozzles with Mach 3 and Mach 3.5 and for the advanced Mach 3.5 axisymmetric quiet nozzle over the unit Reynolds number range tested. For each nozzle, the measured maximum surface roughness k in the throat region is listed to show the effect of surface finish on the performance. For the advanced nozzle, the data indicate that with $k = 2.5\ \mu$m the quiet flow is completely lost for $Re_\infty/\text{m} > 2.2 \times 10^7$ ($Re_\infty/\text{ft} > 6.7 \times 10^6$); when $k = 2.0\ \mu$m, a quiet test core exists up to about $Re_\infty/\text{m} \sim 3.5 \times 10^7$ ($Re_\infty/\text{ft} \sim 11 \times 10^6$) beyond which the quiet test core again disappears. The loss of quiet test core is due to the loss of laminar flow on the nozzle wall. The data in Fig. 1 suggest that the laminar–turbulent transition on the nozzle wall is linked to the surface roughness in the nozzle throat region. The computational results we report in this paper rule out some of the other possible reasons for the loss of laminar flow. Hence, in this paper we focus on roughness-induced transition and the control technique of throat heating.

Received 9 May 2002; revision received 18 September 2002; accepted for publication 5 November 2002.

*Research Scientist; currently Senior Research Engineer, Noise and Vibration, Systems Department, United Technologies Research Center, East Hartford, CT 06108. Member AIAA.

†Senior Research Scientist; currently Aerodynamics Section Supervisor, Lockheed Martin LaRc Program Office, Hampton, VA 23681. Senior Member AIAA.

‡Chief Scientist. Associate Fellow AIAA.

Investigations[2,3] on the effect of two-dimensional and distributed surface roughness on the transition from laminar to turbulent flow had been conducted in the early 1960s. It was found that the existence of the roughness elements on a surface can either introduce no disturbances of sufficient magnitude to influence transition or, beyond a threshold of height, causes transition to move substantially up to the element itself. The data from several low-speed investigations, for example, Refs. 4–8, of three-dimensional roughness indicated that the onset of transition can be correlated with the roughness Reynolds number Re_k ($= u_k \cdot k/\nu_k$), based on roughness height k, boundary-layer velocity u_k at height k (in the absence of roughness), and the kinematic viscosity ν_k at the height k above the wall. In these studies, critical value of Reynolds number Re_k was found to be 400. However, based on experience with the pilot quiet nozzles, it has been suggested by Beckwith et al.[9] that the value of $Re_k = 12$ should be used as the criterion of allowable surface roughness for the design of supersonic quiet tunnels.

Note that the critical roughness Reynolds number is defined as the Reynolds number above which transition onset location is severely impacted. In contrast, the effective roughness Reynolds number is the Reynolds number at which transition location moves into the vicinity of the roughness. The value of $Re_k = 12$ suggested by Beckwith et al.[9] is the critical roughness Reynolds number based on the height of a single roughness peak and not the rms roughness distribution. This is because a single outstanding roughness can cause "localized" transitional flow, which can spread and contaminate the surrounding boundary-layer flow. Thus, based on the criterion of Beckwith et al., the maximum allowable peak-to-valley roughness height for the advanced Mach 3.5 axisymmetric quiet nozzle should be less than $1.2\ \mu$m in the throat region to achieve the design value of Reynolds number $Re_{\Delta x}$ at higher values of Reynolds number Re_∞. This possibly explains why laminar flow on the nozzle wall was completely lost in the advanced Mach 3.5 axisymmetric quiet nozzle when the freestream unit Reynolds number was raised beyond $Re_\infty/\text{m} \sim 3.5 \times 10^7$ ($Re_\infty/\text{ft} \sim 11 \times 10^6$).

The determination of the critical roughness height must fully rely on empirical formulas, for example, $Re_k = 12$, for high-speed quiet tunnels. This is the criterion we use for the present study. However, note that the criterion suggested in Ref. 9 is based on limited number of tests, and the accuracy and general validity of the roughness data are by no means established. Therefore, the available roughness data can be considered to represent only estimates or guidelines for fabrication.

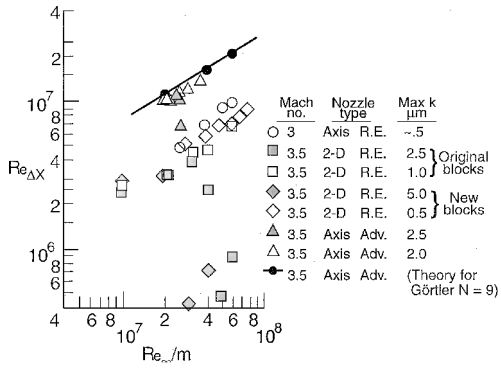

Fig. 1 Quiet test core Reynolds numbers in the advanced Mach 3.5 axisymmetric quiet nozzle (Adv.) and pilot quiet nozzles (R.E.) (from Ref. 1).

In general, the requirements of surface finish in the critical throat region become more stringent with thinner boundary layers as the operational unit Reynolds number increases. A high-quality surface finish can dramatically increase the construction cost of the nozzle, if not make manufacturing and maintenance impossible. To increase roughness tolerance, techniques such as throat heating have been proposed by Harvey et al.[10] The idea is to use wall heating to thicken the boundary layer in the throat region, and as a result, a given roughness height will yield a lower roughness Reynolds number. Therefore, the surface finish specification may be relaxed.

The effect of throat heating on the state of boundary-layer needs to be carefully examined. It is well known that wall heating (in air) destabilizes Tollmien–Schlichting (T–S) waves in the flat-plate boundary layer, but, in the throat region, strong favorable pressure gradients cancel the adverse effect of heating and the boundary layer is expected to remain stable to T–S waves. However, as will be demonstrated later, throat heating could destabilize the boundary layer to high-frequency inviscid disturbances, which could in turn cause early transition. Hence, to take full advantage of throat heating without destabilizing the flow, the overall effect of throat heating must be carefully evaluated. We note that throat heating was utilized by Schneider[11] in the design of a Mach 6 quiet nozzle, with the main objective of transition delay by providing downstream cooling effect in the sense of Dovgal et al.[12] The effect of throat heating has also been studied by Demetriades,[13] albeit in a different context.

In this paper, we consider effectiveness of throat heating on increasing roughness tolerance for two advanced axisymmetric nozzles. In the first case, results of the analysis for a Mach 3.5 axisymmetric quiet nozzle are presented. In the second case, results of a similar analysis for a Mach 2.4 nozzle are given. In these two cases, the maximum allowable amount of heating and the corresponding critical roughness heights are identified when the nozzles are operating at their highest design conditions. We also investigate the effect of heating on the stability of the nozzle wall boundary layers, which are otherwise stable in the throat region due to strong favorable pressure gradients. It is found that throat heating could bring about an inviscid instability if the heating level is sufficiently high.

II. Nozzle Mean Flow Computations

A. Mach 3.5 Nozzle

For the Mach 3.5 advanced nozzle, the NASA Langley Research Center compressible thin-layer Navier–Stokes code CFL3D[14] was used to obtain the flow solution for the entire nozzle, including the subsonic approach, at the condition of $Re_\infty = 10 \times 10^6$/ft ($3.3 \times 10^7$/m). It is assumed that the boundary layers on the wall of subsonic approach section and the wall of the bleed slot are turbulent. This nozzle lost its entire quiet test core suddenly when freestream (or unit) Reynolds number was increased beyond a certain critical value. To understand fully this loss of laminar flow, it was desired to compute the flowfield around the nozzle lip hoping that it may provide some clues. Two questions needed to be answered. First, is the turbulent boundary layer on the subsonic approach fully swallowed by the suction slot or does part of it spills over to the nozzle lip? Second, can the flow topology near the nozzle lip support a separation bubble? To provide definitive answers to such concerns, the actual geometry of the subsonic approach including the suction slot and the entire nozzle contour from suction lip to exit of the nozzle was used to generate a multiblock grid to facilitate a full blown computational fluid dynamics computation using CFL3D.

1. *Grid Topology*

To facilitate the computation, a multiblock grid was generated. The global geometry used for computation includes a substantial portion of the upstream region; the inflow area is extended up to that of the settling chamber. In the downstream direction, the present computational region covers the entire nozzle geometry. In consideration of the boundary-layer bleed slot, it was decided to use a multizone grid topology generated by grid-generation software GRIDGEN. This enabled better control of grid points and resolution of the rapidly growing boundary layer.

The computational domain fully represents the actual geometry of the tunnel (Fig. 2). We set the inflow boundary at 8.39 in. upstream of the throat with a radius of 6.59 in. The inflow Mach number varies from 0.025 near the wall to 0.055 in the core. Spline smoothing was applied to the subsonic convergent wall shape in view of the relatively small number of tunnel wall coordinates available. The supersonic portion of the nozzle geometry was found to have small point-to-point variations resulting in small oscillations in the curvature distribution. Spline interpolation followed by five cycles of five-point smoothing was used to ensure that the wall curvature has the minimum desired degree of smoothness required for numerical solution.

To resolve adequately the flow around the bleed inlet region better, a complicated grid topology was successfully implemented; Fig. 3 shows various zones. The suction lip region around the bleed slot now has a wraparound C-type grid. This grid is smoothly connected to an H-type grid topology elsewhere in the flow. This was accomplished with the GRIDGEN suite of grid-generation software. The wall boundary-layer regions are now separate zones, which enable flexibility in adjusting grid resolution, which can be easily accomplished by changing the number of points in those zones. Overall,

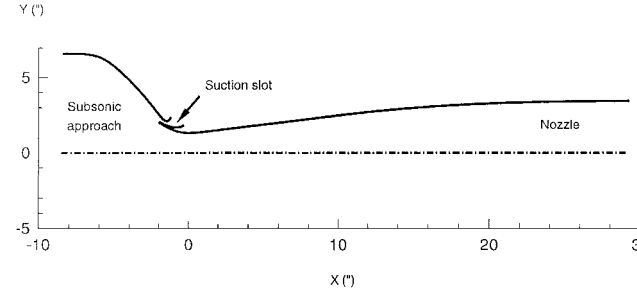

Fig. 2 Mach 3.5 axisymmetric nozzle geometry including subsonic approach and suction slot.

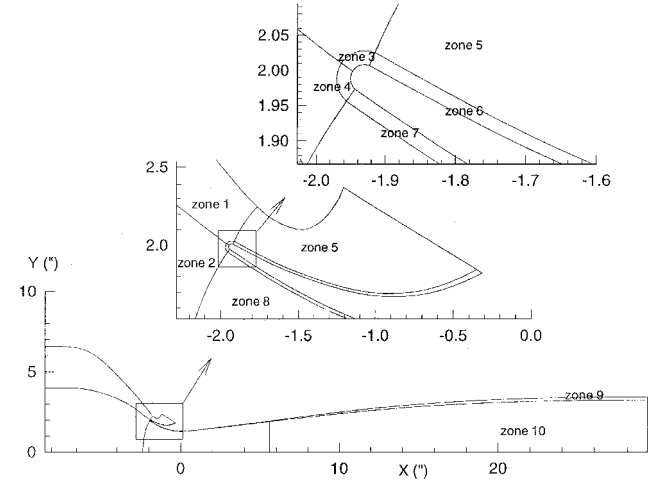

Fig. 3 Zones for the Mach 3.5 axisymmetric nozzle computational grid.

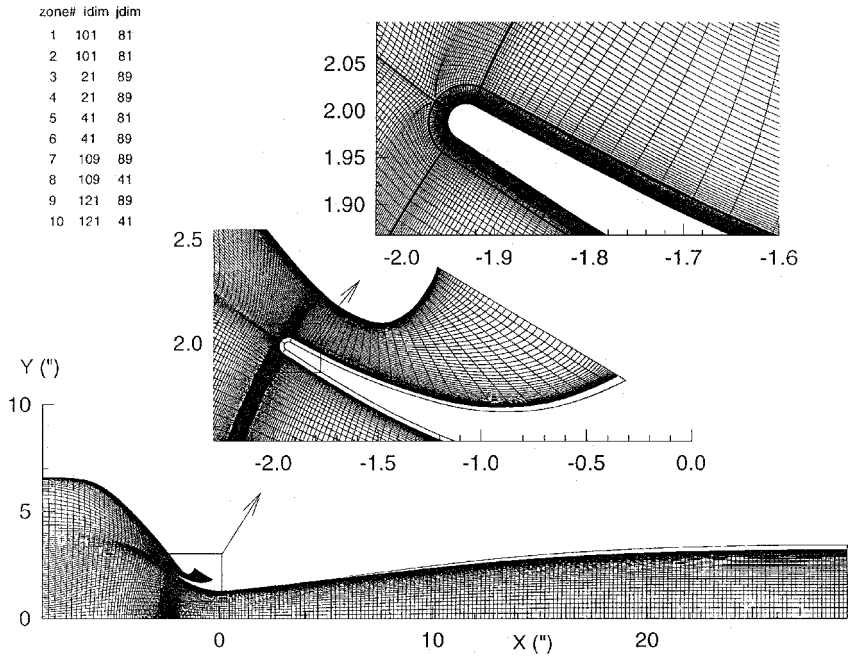

Fig. 4 Details of computational grid: *i*dim and *j*dim indicate number of grid points in *x* and *y* directions.

the entire flowfield is described by 10 connected zones. Figure 4 shows the grid distribution employed in all zones. Preliminary coarse grid computations were helpful in determining the variation of boundary-layer thickness; this information was then used to refine the grid so that velocity profiles and their derivatives are adequately defined (Sec. II.A.3). In this study, we typically place about 40–70 grid points within the boundary layer.

Details of the grid points used in various zones is as follows. The subsonic approach region is divided into zones 1 and 2, each containing 101×81 grid points with the latter number indicating grid points in the wall-normal direction. Zones 3 and 4 (each with 21×89 grid points) cover the circular portion of the nozzle lip. Zone 5 and zone 6 are placed inside the suction slot, and they have 41×81 and 41×89 grid points, respectively. Zone 7, which has 109×89 grid points, lies near the wall of converging/diverging nozzle and starts at the end of zone 4 and extends up to about $x = 5.5$ in. Zone 8, with 109×41 points, covers the inviscid region and extends up to the same x location. Finally, zones 9 (with 121×89 points) and 10 (with 121×41 points) are placed in the near-wall viscous region and the inviscid core region of the nozzle for $x > 5.5$ in.

2. *Nozzle Flowfield*

The Navier–Stokes solution for the entire nozzle was obtained for a Reynolds number based on Mach 3.5 conditions, that is, at the nozzle exit, of 10×10^6/ft (3.3×10^7/m) using the CFL3D code. Total temperature is 540°R, and Sutherland viscosity law is employed. The boundary conditions used in the CFL3D computations are as follows: 1) inflow with specified total conditions in the subsonic approach, 2) extrapolation boundary condition at the supersonic nozzle exit and the suction slot exit (because the flow in the suction slot is also chocked), and 3) no-slip conditions at all solid boundaries with either adiabatic wall or specified wall temperature. Whereas it was assumed that the boundary layers on the wall of the subsonic approach section and the wall of the bleed slot are turbulent, the boundary layer on the nozzle inner wall starting from the rounded lip was assumed to be laminar. Convergence was assured by driving the residuals down to 10^{-9} and by monitoring the velocity and temperature profiles near the nozzle exit plane where the solution is the slowest to settle to a steady state. Iterations in excess of 30,000 were carried out to ensure full convergence. The convergence history is shown in Fig. 5.

Figure 6 shows contours of the Mach number. We note that the design value of $M = 3.5$ is reached at the nozzle centerline at about

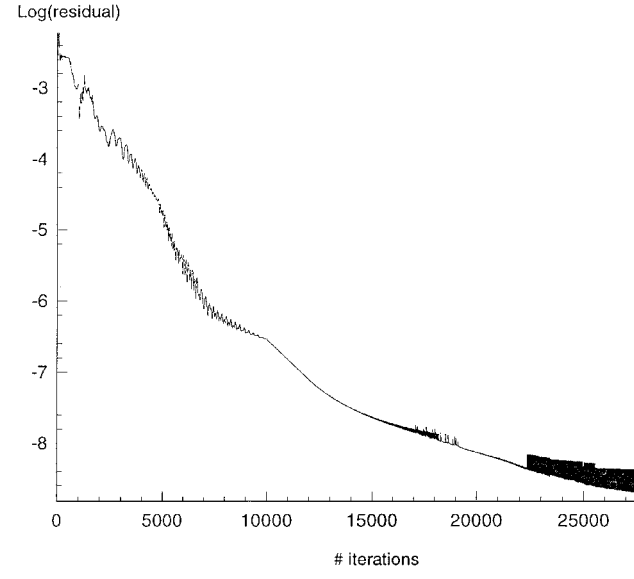

Fig. 5 Convergence history for the $Re = 10 \times 10^6$/ft (3.3×10^7/m) case using CFL3D.

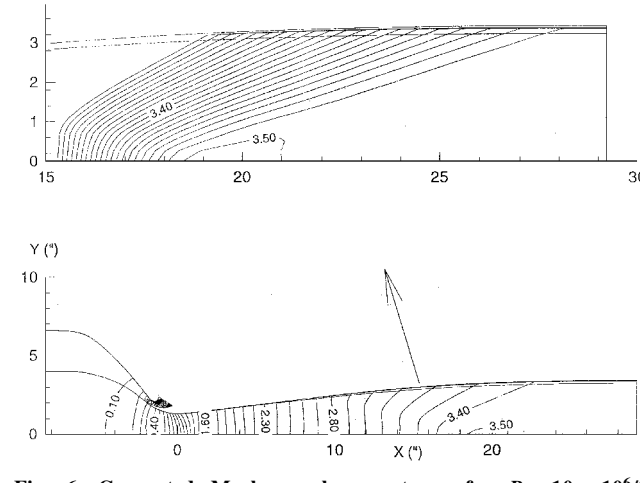

Fig. 6 Computed Mach number contours for $Re = 10 \times 10^6$/ft (3.3×10^7/m) case.

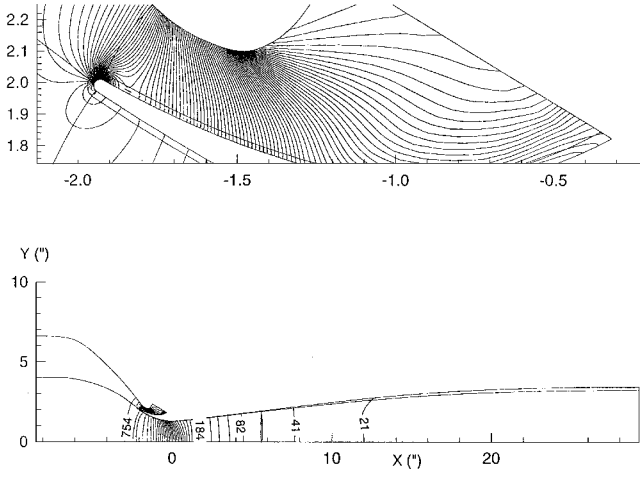

Fig. 7 Computed pressure contours for $Re = 10 \times 10^6$/ft (3.3×10^7/m) case.

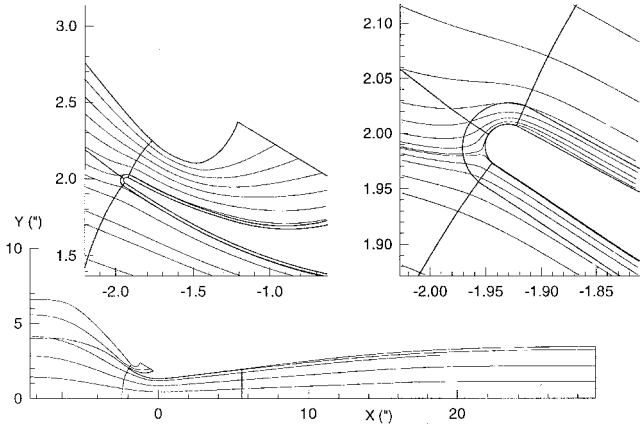

Fig. 8 Computed streamline traces for the $Re = 10 \times 10^6$/ft (3.3×10^7/m) case and grid zonal boundaries.

21 in. from the throat, or 8.2 in. upstream of the nozzle exit plane. Figure 7 shows the pressure contours in the nozzle, with a closeup of the bleed slot region, which indicates the location of the stagnation point. Figure 8 shows streamline traces in the nozzle and a closer look at the streamlines around the bleed slot. It is clear that the stagnation point is on the lower part of the rounded lip and that the flow in the lower portion of the nozzle lip is somewhat similar to the flow on the lower surface of an airfoil at incidence, which ensures an attached laminar flow on the nozzle wall. Hence, it is concluded that the flow around the nozzle lip region is free from any anomaly that might have affected the development of the new laminar boundary layer in the nozzle. An examination of the boundary-layer profiles also revealed that the turbulent boundary layer on the subsonic approach was fully swallowed by the suction slot. We note that, although the results in Figs. 7 and 8 show that the flow on the inner side of the nozzle lip is attached, the possibility of a separation bubble on the suction-slot side cannot be ruled out in view of the adverse pressure gradient region evident from pressure contours of Fig. 7. However, we have not investigated this possibility with a fine-enough grid in zone 6 to make any definite conclusion.

We note that the applicability of the thin-layer Navier–Stokes solver may be open to questions in the rounded (circular) region of the nozzle lip. However, we know that the flow near the stagnation point (line) can be approximated by the Hiemenz flow in the incompressible case, where $u = cx$, that is, $u_{xx} = 0$. Therefore, the thin-layer approximation in the neighborhood of the stagnation line is not without justification, provided the x direction is carefully selected, that is, the x direction is tangent to the surface.

3. Boundary-Layer Computations

Before linear-stability analysis is started, it is important to ensure that the boundary-layer profiles, obtained from the Navier–Stokes computations, are physically realizable. One way to ascertain this is to perform a grid convergence study, that is, doubling and tripling the number of grid points and observing the change in solution behavior. This is clearly a computationally intensive task for a Navier–Stokes code. Therefore, we adopt an alternative approach in this study. We argue that because no significant viscous/inviscid interaction is expected for the circular nozzle flow, the solution obtained by solving boundary-layer equations is the physically relevant solution in the vicinity of the nozzle wall. Then, if the Navier–Stokes solution near the wall agrees with the boundary-layer solution, we can accept the former as an adequately resolved viscous solution for the converging/diverging supersonic nozzle. This is the approach adopted here.

We compare the Navier–Stokes profiles in zones 7 and 9 with boundary-layer solution obtained by the code developed by Harris and Blanchard.[15] For this purpose, the surface pressure was extracted from the Navier–Stokes solution; a five-cycle, five-point smoothing was applied to the pressure distribution to eliminate any small point-to-point "noise" in the pressure distribution. Then a boundary-layer calculation was performed based on the smoothed pressure distribution. Figure 9 shows this comparison for streamwise velocity, wall-normal velocity, temperature, and density at the following locations: $X = 0.013$, 0.099, 0.31, 0.63, 0.97, 1.3, 1.63, 1.95, 2.28, and 2.56 ft from the nozzle throat. Because there is negligible viscous inviscid interaction in the present case, the two sets of profiles are almost identical as expected. Therefore, we conclude that the boundary-layer grid used in the Navier–Stokes computation is adequate. The agreement between boundary-layer solution and Navier–Stokes solution upstream of the throat, although not shown, was also reasonably good. We note that boundary-layer equations are written in similarity variables that reduce the equations to ordinary differential equations at the stagnation line. The latter were solved to provide initial conditions for marching solutions of the parabolic partial differential equations.

Throat heating analysis would require boundary-layer profiles for several values of unit Reynolds numbers. Because the CFL3D calculation is not only computationally intensive but also requires adjustment of grid for proper resolution of the boundary layers, we considered an alternative simplified approach. To perform the current investigation in an expeditious manner, the wall pressure variation obtained from the $Re_\infty = 10 \times 10^6$/ft ($3.3 \times 10^7$/m) Navier–Stokes solution was scaled up in proportion to the increase in tunnel total pressure. For example, the $Re_\infty = 18 \times 10^6$/ft ($5.9 \times 10^7$/m) case was obtained by scaling up wall pressure by a factor of 1.8 and then performing an axisymmetric boundary-layer calculation by using

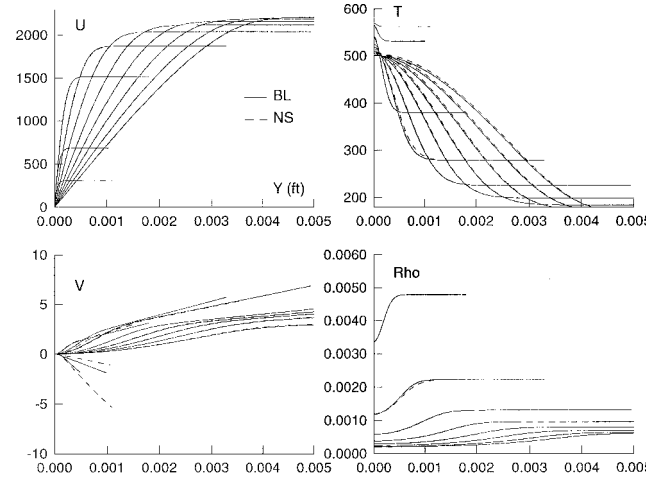

Fig. 9 Comparison of velocity, temperature, and density profiles from the CFL3D computation and an axisymmetric boundary-layer computation, which used smoothed wall pressure distribution extracted from the CFL3D solution, at $X = 0.013$, 0.099, 0.31, 0.63, 0.97, 1.3, 1.63, 1.95, 2.28, and 2.56 ft from the nozzle throat.

the boundary-layercode. Similarly, the $Re_\infty = 25 \times 10^6$/ft case was obtained by a scale up of 2.5. Only the pressure and density vary with change in total pressure; all other quantities including edge Mach number and wall temperature are assumed to remain unchanged.

B. Mach 2.4 Pilot Nozzle

For the Mach 2.4 axisymmetric pilot nozzle, the mean flow computation was done by a two-dimensional/axisymmetric compressible Navier–Stokes code HTC2D. In this case, the boundary-layer solution needed for linear stability analysis was directly resolved in the Navier–Stokes computation. In the HTC2D code, Navier–Stokes (N–S) equations are discretized in a vertex-based control volume fashion with $(\rho, u, v, e)^T$ as the independent variable vector. For the inviscid fluxes, a low-diffusion flux-splitting scheme is used, whereas the viscous fluxes are discretized using a second-order accurate three-point stencil. To achieve fast convergence to steady state, the full multigrid–full approximation storage scheme is used. Detailed descriptions about a three-dimensional version of the code, including accuracy, efficiency, and code validation have been documented in Refs. 16 and 17 and will not be discussed here.

III. Linear Stability Analysis

It is well known that, in a RE nozzle, Görtler instability in the wall boundary layer can lead to the transition from laminar to turbulent flow. The e^N calculations[18] based on a linear quasi-parallel stability theory indicated that the transition onset location could be well correlated with an N factor of about 9–11 for a range of unit Reynolds numbers (3×10^6/ft $\sim 18 \times 10^6$/ft). Görtler instability, being a curvature-induced instability, is difficult to control with wall suction or cooling; the most effective way to control Görtler instability is to reduce the concave curvature by adopting a slow expansion configuration, that is, a longer nozzle. Beckwith et al.[19] designed a long slow expansion nozzle that could yield much longer quiet test core. However, in a longer nozzle with a weakened favorable pressure gradient, the T–S instability can become relevant. As will be shown later, a new type of instability that is inviscid in nature could also become relevant and cause premature breakdown of laminar boundary layer when the nozzle throat is heated. Because of the existence of these competing instabilities, an optimal nozzle design can only be achieved when all of them are considered thoroughly.

In the present work, stability analysis and N-factor calculations are performed by using the linear stability code eMalik2D, which solves the spatial eigenvalue problem associated with the compressible linear stability equations and is capable of handling both T–S (viscous/inviscid) and Görtler disturbances under quasi-parallel approximation. In the quasi-parallel approximation, the effect of boundary-layer growth is assumed to be a higher-order effect and, hence, neglected. Details of the compressible stability equations and the numerical method used in this stability code have been given in Ref. 20. Before we present the major results of this paper, we must caution against the use of stability theory for transition prediction in flow with sufficiently large roughness where the stage governed by linear theory may be completely bypassed. Furthermore, the use of parallel approximation introduces an unknown error in the results, and this approximation can only be justified by comparing against computational results where nonparallel effects are not ignored.

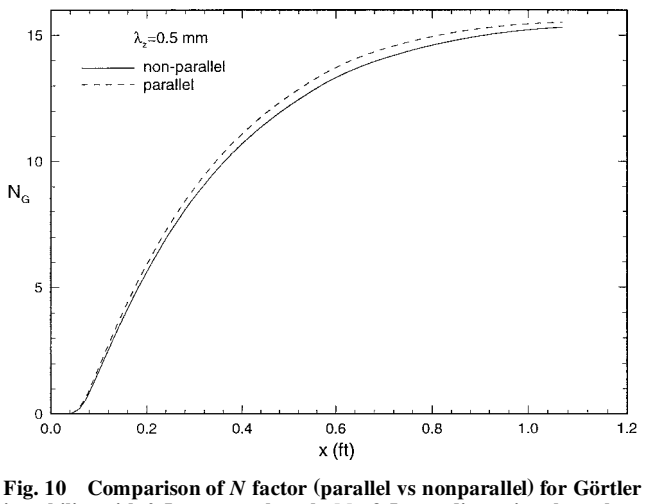

Fig. 10 Comparison of N factor (parallel vs nonparallel) for Görtler instability with 0.5-mm wavelength, $M = 3.5$, two-dimensional nozzle.

To assess the effect of nonparallelism, we have performed a calculation for the two-dimensional Mach 3.5 nozzle considered in Ref. 18. Figure 10 is a comparison of Görtler N factors computed using quasi-parallel theory (eMalik2d) and nonparallel theory [linear parabolized stability equations (PSE)] for the most amplified Görtler wavelength of 0.5 mm for the selected flow conditions, $Re_\infty/\text{m} = 20 \times 10^6$ ($Re_\infty/\text{ft} = 6.1 \times 10^7$). The Görtler N factor (using PSE) at the transition location of $X = 0.32$ is 9.2. This number can be compared with $N = 9.6$, which was obtained by Chen et al.[18] When it is considered that Chen et al. used quasi-parallel theory in conjunction with boundary-layer solution, whereas the present PSE calculation accounts for nonparallel effect and uses N–S mean flow, the agreement between the present computation and that of Chen et al. is quite good. The results presented in Fig. 10 show that the nonparallel effect is small, which is a consequence of relatively large values of Görtler number associated with this nozzle wall boundary layer. Note that, for Görtler vortices, the nonparallel effect is stabilizing. This conclusion was also reached by Spall and Malik.[21] We should caution here that the relatively small effect of nonparallelism noted is specific to the conditions of the cited supersonic nozzles. This should not be taken as a general conclusion for the effect of mean flow variation on the Görtler instability or other boundary-layer instabilities.

IV. Effect of Throat Heating

A. Mach 3.5 Advanced Nozzle

As noted earlier, our N–S calculations indicate that the turbulent boundary layer in the subsonic approach to the nozzle is completely removed by the suction slot upstream of the throat, and a new laminar boundary layer begins to develop downstream of the slot without any anomalous behavior. Therefore, to explain the loss of quiet test zone (Fig. 1) with increase in unit Reynolds number beyond 3.5×10^7/m ($\sim 11 \times 10^6$/ft), attention is focused on roughness-induced transition near the nozzle throat.

For the throat heating for controlling roughness-induced transition, calculations were done with different levels of heat transfer to determine the acceptable limit. The cases studied and the conditions considered are summarized in Table 1.

As mentioned earlier, throat heating can destabilize the wall boundary layer. The effect of heat transfer on the instability of compressible boundary layers has been studied by many researchers. Using inviscid and viscous theories, Mack[22,23] found that, whereas surface cooling stabilizes first-mode waves, it destabilizes second-mode instability. For moderate Mach numbers, cooling can be applied to remove the generalized inflection point, which is defined as the point inside the boundary layer where $\mathrm{D}(\rho \mathrm{D}u) = 0$ and is the source of the first-mode instability. For the nozzles studied in this paper (Mach 3.5 and Mach 2.4), the first mode and the Görtler instabilities are the relevant perturbations. In contrast to surface cooling, it can be expected that uniform heating will destabilize the first-mode disturbance in nozzle wall boundary layer, although the favorable pressure gradient present in the throat region has a stabilizing influence. We note that experiments of Demetriades[13] showed that transition was delayed in his nozzle with throat heating, although the source of instability causing transition remained obscured.

The stability behavior of a boundary layer can be deduced by studying the effect of heat transfer on the mean flow characteristics. An important feature of the compressible boundary layer on a

Table 1 Throat heating conditions considered for the advanced Mach 3.5 axisymmetric quiet nozzle

		$T_{\text{wall}}/T_{\text{ad}}$				
$Re_\infty/\text{ft} \times 10^{-6}$	Heated domain, ft	1	1.3	1.7	1.9	2.2
10	$x < 0.10$	×	×			
18	$x < 0.15$	×		×	×	
25	$x < 0.20$	×		×	×	×

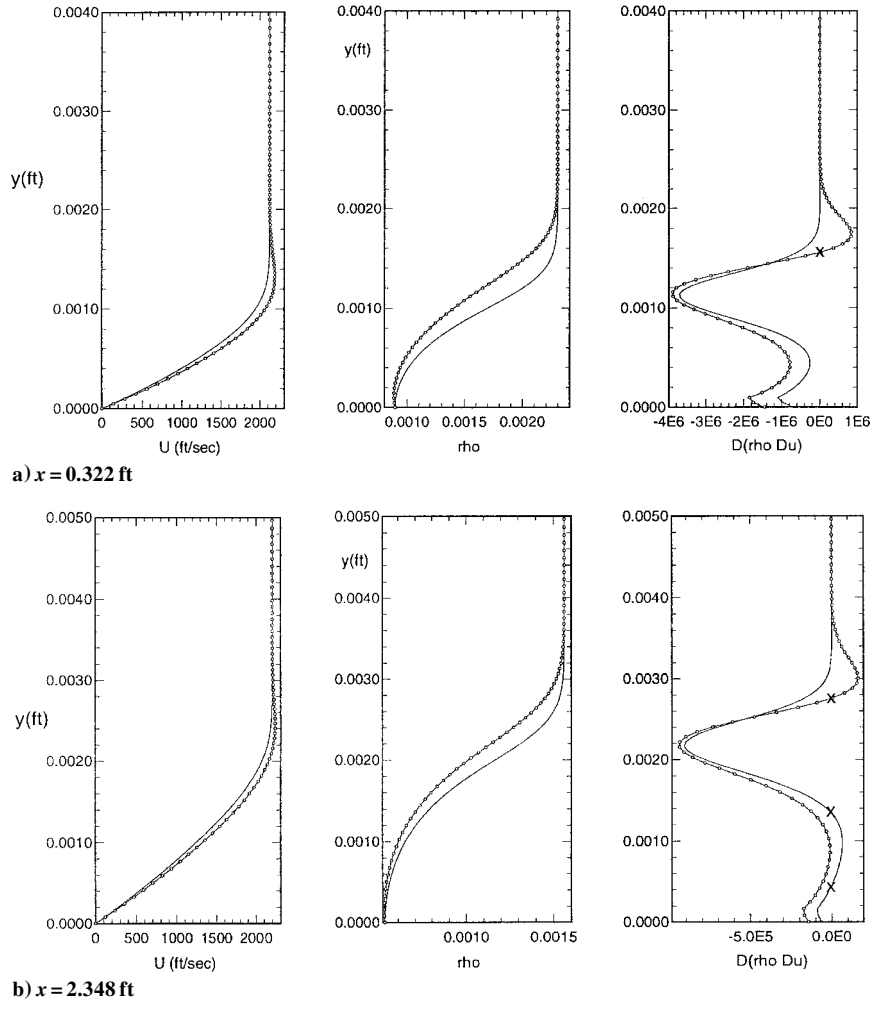

Fig. 11 Comparison of streamwise velocity u, density ρ, and D(ρDu), that is, d/dy[ρ(du/dy)], distributions in the wall normal direction for $Re_\infty = 25 \times 10^6$/ft: ——, adiabatic wall; ○, $T_w = 2.2T_{ad}$ for $x < 0.2$ ft; and ×, generalized inflection points.

flat plate is the existence of a generalized inflection point, that is, $\mathrm{d}/\mathrm{d}y[\rho(\mathrm{d}u/\mathrm{d}y)] = 0$, where ρ is the local density, u the boundary-layer velocity, and y the wall-normal coordinate inside the boundary layer, which makes the boundary layer unstable to inviscid disturbances. Wall cooling tends to eliminate this inflection point making the boundary layer less susceptible to inviscid disturbances. Contrarily, sufficient surface heating pushes the generalized inflection toward the edge of boundary layer and enhances inviscid instability. For the adiabatic wall case, boundary-layer profiles in the throat region are free from generalized inflection points due to strong favorable pressure gradients. Therefore, this boundary layer is free from inviscid first-mode type disturbances. However, the combined effect of flow acceleration (negative pressure gradients) and wall heating results in an overshoot in the streamwise velocity profile as earlier found by Cohen and Reshotko.[24] This is because the low-density gas near the wall is accelerated more strongly by the external pressure gradients in the case of wall heating. The velocity overshoot gives rise to an inflection point making the boundary layer susceptible to inviscid disturbances. Figures 11a and 11b show the velocity and density profiles as well as the quantity $\mathrm{d}/\mathrm{d}y[\rho(\mathrm{d}u/\mathrm{d}y)]$ at $x = 0.322$ and 2.348 ft (where $x = 0$ coincides with the throat), when $Re_\infty = 25 \times 10^6$/ft and a wall temperature $T_w = 2.2T_{ad}$ is applied up to $x < 0.2$ ft. Except for the heated region, the wall temperature is assumed to remain at its previous adiabatic wall temperature. (This implies wall cooling.)

Boundary-layer profiles (velocity u and density ρ) and the quantity $\mathrm{d}/\mathrm{d}y[\rho(\mathrm{d}u/\mathrm{d}y)]$ at location $x = 0.322$ are presented in Fig. 11a. For the sake of discussion, we designate $\mathrm{d}/\mathrm{d}y[\rho(\mathrm{d}u/\mathrm{d}y)]$ as Λ here. For a compressible flat-plate boundary layer with an adiabatic wall boundary condition, Λ has one zero; for a moderately cold wall, Λ has two zeros inside the boundary layer, and it is the outer of these two that gives rise to the inviscid first-mode instability that is more amplified for oblique waves. For very cold walls, Λ has no zeros within the boundary layer, and therefore, the boundary layer is free of first-mode disturbances. For the present adiabatic wall case, Λ does not assume the value 0 inside the boundary layer, which is a consequence of the strong favorable pressure gradient, and hence, this boundary layer is free from inviscid instabilities. In Fig. 11b, results are presented at $x = 2.348$. Because at this location pressure gradient is relatively weak, Λ has two zeros inside the boundary layer. Therefore, the possibility of first-mode disturbances exists at this location for the adiabatic wall case.

Now, let us discuss the results in the presence of throat heating. In Fig. 11a, we note that the velocity profile has a slight overshoot near the edge of the boundary layer that results in a zero crossing for Λ at $y \approx 0.00175$ ft. This zero crossing (or generalized inflection point) is also present at $x = 2.348$ (Fig. 11b). We shall see that associated with this inflection point will be an inviscid instability. We note here that, close to the wall, the Λ curve has been pushed away from the zero line for the case with throat heating. In Fig. 11b, it can be seen that the two inflection points ($\Lambda = 0$) near the wall present in the adiabatic wall case are no longer present for the case with throat heating. The elimination of the two inflection points near the wall is a consequence of the implicit wall cooling that follows the heating strip. This wall cooling downstream of a heating element was found to stabilize T–S waves by Dovgal et al.[12] in the context of low-speed flow over a flat plate.

Three observations can be made from the described mean flow profiles: 1) Because the new inflection point lies near the edge of the boundary layer, we expect the phase speed of the inviscid instability

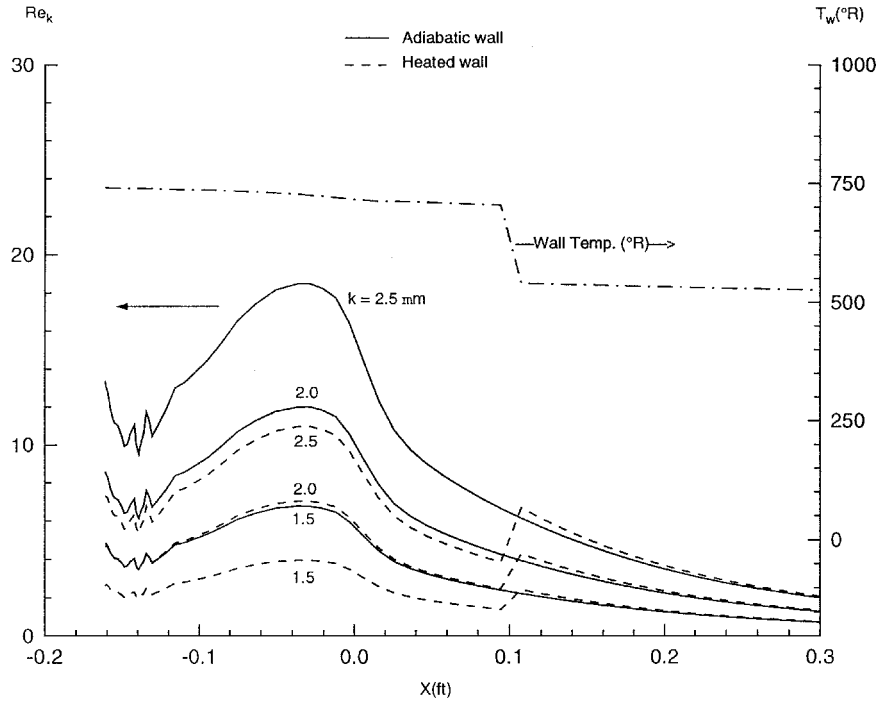

Fig. 12 Distribution of Reynolds number Re_k for various fixed roughness heights, $k = 2.5$, 2.0, and 1.5 μm, using $Re_\infty = 10 \times 10^6$/ft ($3.3 \times 10^7$/m) for adiabatic wall and throat heating case ($T_w = 1.3T_{ad}$).

to be close to 1.0 when scaled with the freestream velocity. 2) If the boundary-layer thickness is assumed to be a good approximation of the length scale for the inviscid instability, then in this case the inviscid instability due to throat heating will have a very high frequency, on the order of 1000 kHz (or 1 MHz). 3) Because the relative speed between the disturbance and the mean flow near the edge of boundary layer is low subsonic ($|U_e - c_r|/a \ll 1$), we expect the inviscid instability to be dominated by two-dimensional disturbances unlike the first-mode disturbances, which are most amplified when oblique. As will be shown later, results of the stability analyses are all in agreement with these conjectures.

Figure 12 shows the Reynolds number Re_k values for an adiabatic wall and for a heated wall with $T_w = 1.3T_{ad}$ in the range of $-0.12 < X < 0.1$ ft when $Re_\infty = 10 \times 10^6$/ft ($3.3 \times 10^7$/m). Also shown in Fig. 12 is wall temperature distribution. The heating corresponds to a temperature rise of approximately 125°R. The streamwise extent of heating strip must cover a region in which the Reynolds number Re_k curve has a peak. For the adiabatic wall ($T_w = T_{ad}$) case, it is noticed that the peak Reynolds number Re_k occurs in a region slightly upstream of the throat. With a roughness height of $k = 2.0$ μm, the peak Reynolds number Re_k is slightly less than the critical value of 12. For the heated case ($T_w = 1.3T_{ad}$), the peak Reynolds number Re_k of the pilot nozzle, which has a roughness height of $k = 2.5$ μm, reduces from 18 to 10. We note that for this relatively low level of heating no inviscid instability is found for this case. All stability results presented in this paper utilize viscous, compressible linear stability theory.

In Figs. 13 and 14, we show the stability results corresponding to wall heating $T_w = 1.9$ and $1.7T_{ad}$, respectively, in the region of $-0.12 < X < 0.15$ ft for $Re_\infty = 18 \times 10^6$/ft ($5.9 \times 10^7$/m). (We note that, based on the data in Fig. 1, the advanced nozzle had already lost the quiet test core before arriving at this freestream condition.) Comparing Figs. 13 and 14, we note that the throat heating has a negligible effect on the Görtler instability, which does not become unstable until farther downstream from the heated throat region. In these two cases, it is clear that heating has introduced a new two-dimensional (or, in the present case, an axisymmetric) instability, which is caused by the inflectional nature of the mean flow profile, and the most unstable disturbance has a frequency around 1000 kHz. Although not shown here, the nondimensional phase speed of this unstable mode is slightly greater than 1 because the inflection point occurs at a location where velocity is higher than the outer flow velocity. It may

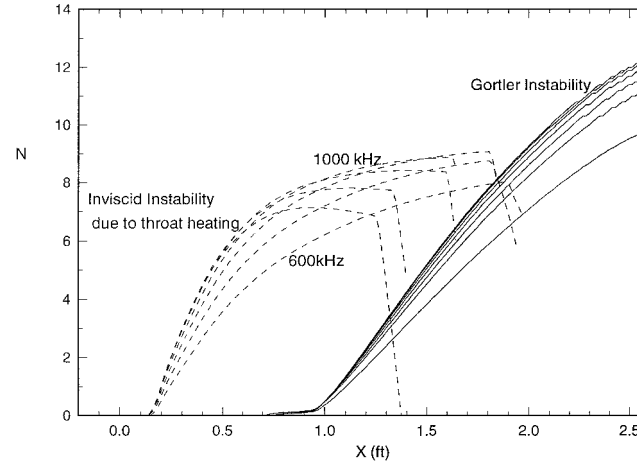

Fig. 13 Computed N values for Görtler vortices and heating-induced inviscid instability for $Re_\infty = 18 \times 10^6$/ft ($5.9 \times 10^7$/m) and $T_w = 1.9T_{ad}$ for $x < 0.15$ ft.

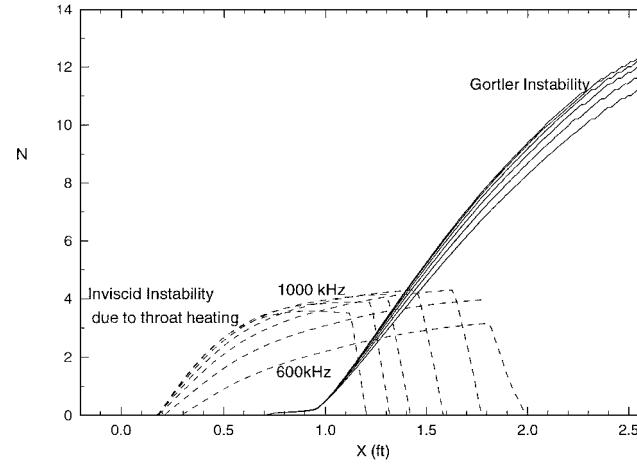

Fig. 14 Computed N values for Görtler vortices and heating induced inviscid instability for $Re_\infty = 18 \times 10^6$/ft ($5.9 \times 10^7$/m) and $T_w = 1.7T_{ad}$ for $x < 0.15$ ft.

be argued that the oncoming stream would be devoid of very-high-frequency [$\mathcal{O}$(1 MHz)] disturbances and, therefore, that the boundary layer will have no "input disturbances" to amplify. If that were to be the case, the inviscid instability found here will not necessarily lead to laminar–turbulent transition. Note, however, that available wind-tunnel instrumentation is not capable of measuring such high-frequency disturbances with any reasonable signal-to-noise ratio.

The maximum allowable wall temperature is limited by the associated N factors computed for the inviscid instability. The maximum N factor for the $T_w = 1.9T_{ad}$ case (Fig. 13) reaches a value of about 9 at a location where the corresponding Görtler N factor is only about 4. If the high-frequency disturbance were to be present in the boundary layer, it is likely that they will cause transition well ahead of transition onset location induced by Görtler instability alone. Therefore, it is advisable to limit the growth of the high-frequency instability to a conservative value of N factor, for example, 6. With this criterion, $T_w = 1.9T_{ad}$ is unacceptably high temperature, whereas $T_w = 1.7T_{ad}$ is acceptable. Because $T_w = 1.7T_{ad}$ case yields a N value of 4, perhaps a slightly higher value of T_w will also be acceptable if $N = 6$ is taken as the critical value.

Figure 15 shows the distributions of Reynolds number Re_k for various given roughness heights, for an adiabatic wall and for a wall with a heating strip having $T_w = 1.7T_{ad}$ in the range of $-0.12 < X < 0.15$ ft when $Re_\infty = 18 \times 10^6$/ft ($5.9 \times 10^7$/m). It shows that the heating corresponds to a temperature rise of approximately 350°R. Moreover, with this level of heating the acceptable roughness height increases from slightly below $k = 1.5$ μm to slightly above 2 μm. The 2.5-μm roughness still violates the $Re_k = 12$ criterion. Interpolation of results yield critical k to be 2.2 μm.

Figures 16 and 17 present results of the analyses for the highest design condition of the advanced nozzle, that is, $Re_\infty = 25 \times 10^6$/ft. The level of heating in the range of $-0.12 < X < 0.20$ ft is set at $T_w = 1.7T_{ad}$, which yields inviscid disturbance N factors of about 6 (Fig. 16). If this is accepted to be below the critical value, then the maximum allowable roughness increases from about $k = 0.75$ μm (for the adiabatic case) to k about 1.7 μm, based on interpolation of the results in Fig. 17. Throat heating with $T_w = 1.9T_{ad}$ gave a value of N factor (associated with inviscid disturbances) of 10 at a location where the boundary layer is as yet stable to Görtler instability.

Finally, in Table 2 we summarize the results to highlight the acceptable roughness heights and the level of throat heating for all three cases, Re_∞/ft $\times 10^{-6} = 10$, 18, and 25, considered in this section.

We note that the preceding computations with the heating strip involve a step change in wall temperature. Such a wall temperature distribution can only be maintained if appropriate wall cooling is provided downstream of the heating strip. In the absence of such cooling, axial conduction through the nozzle wall and convection heat transfer will make the nozzle wall temperature decrease gradually downstream of the heating strip. There should not be an appreciable effect of this smooth variation of wall temperature on the Görtler instability and the new high-frequency disturbance. However, the first-mode T–S disturbances may become unstable but not any more than that in the absence of throat heating strip, that is, adiabatic wall temperature all along the nozzle wall.

Table 2 Summary of critical roughness heights and throat heating levels used for the Mach 3.5 axisymmetric nozzle

		Throat heating	
Re_∞/ft $\times 10^{-6}$	Adiabatic condition acceptable k, μm	Level of heating	Acceptable k, μm
10	$k < 2.0$	No need for heating	
18	$k < 1.5$	$1.7T_{ad}$	$k < 2.2$
25	$k < 0.75$	$1.7T_{ad}$	$k < 1.7$

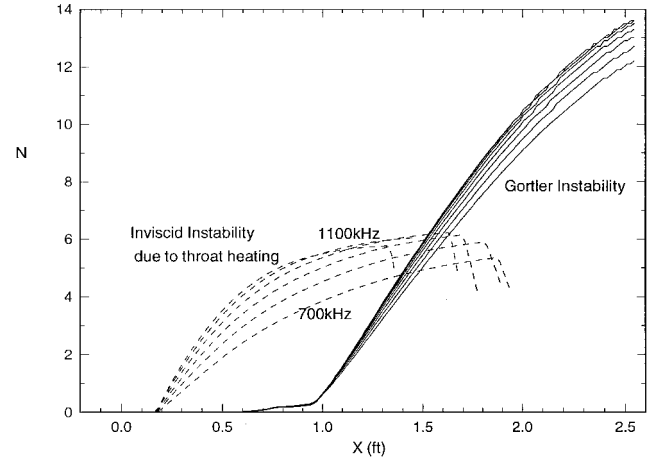

Fig. 16 Computed N values for Görtler vortices and heating induced inviscid instability for $Re_\infty = 25 \times 10^6$/ft and $T_w = 1.7T_{ad}$ for $x < 0.20$ ft.

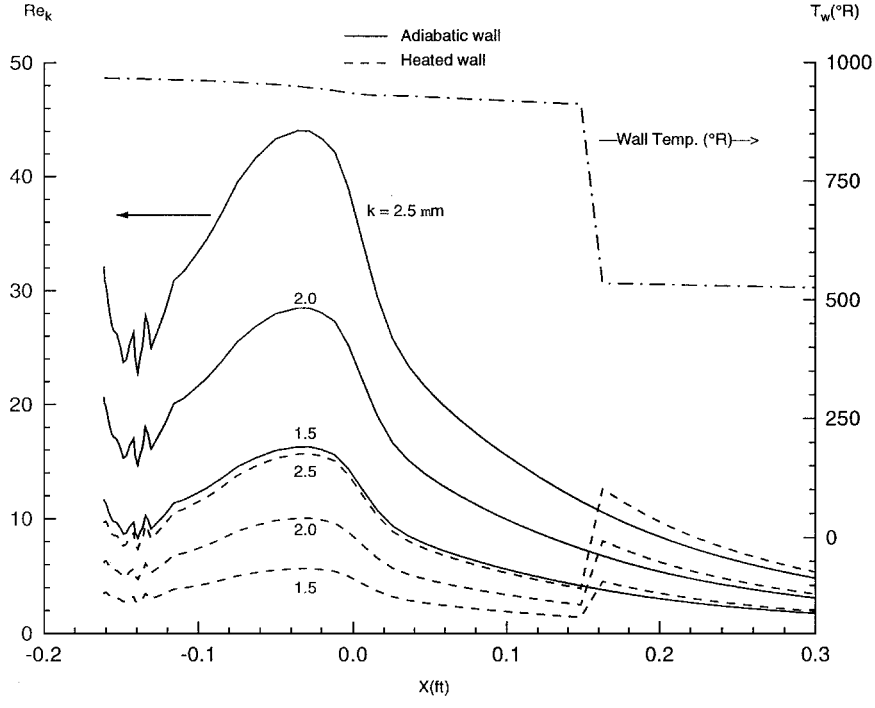

Fig. 15 Distribution of Reynolds number Re_k for various fixed roughness heights, $k = 2.5$, 2.0, and 1.5 μm, using $Re_\infty = 18 \times 10^6$/ft ($5.9 \times 10^7$/m) for adiabatic wall and throat heating case ($T_w = 1.7T_{ad}$).

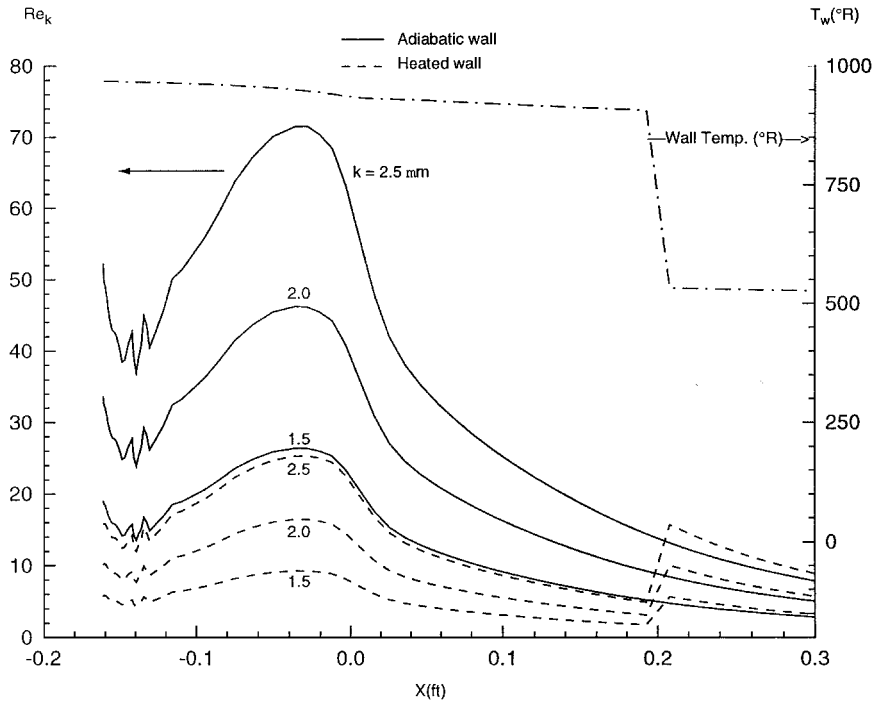

Fig. 17 Distribution of Reynolds number Re_k for various fixed roughness heights, $k = 2.5$, 2.0, and 1.5 μm, using $Re_\infty = 25 \times 10^6$/ft, for adiabatic wall and throat heating case ($T_w = 1.7T_{ad}$).

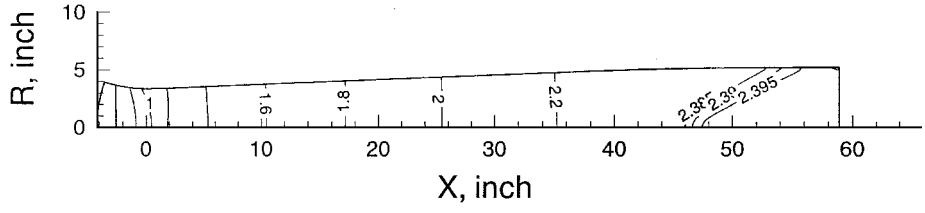

Fig. 18 Mach number contours in the Mach 2.4 axisymmetric pilot nozzle for $T_0 = 540°$ R, $P_0 = 200$ psia, and $T_w = T_{ad}$.

B. Mach 2.4 Pilot Nozzle

This nozzle was designed at NASA Langley Research Center to deliver a quiet test-core-length Reynolds number $Re_{\Delta x} = 80 \times 10^6$, which represents nearly an order of magnitude increase compared to the existing capability. The nozzle we consider in this section is a Mach 2.4 axisymmetric pilot nozzle for the Supersonic Low Disturbance Pilot Tunnel. This pilot nozzle was an attempt at NASA Langley Research Center to demonstrate the feasibility of an ultra-high Reynolds number quiet flow facility. It was anticipated that the technology developed during the design of this pilot nozzle would enable future development of a very large, Mach 2.4 national facility with quiet length Reynolds number capability of 80×10^6. To achieve such high performance, the nozzle must be relatively long. In other words, the nozzle must expand very slowly to limit the growth of Görtler instability. The design also employs an axisymmetric cross section to avoid corner and side wall induced problems and throat heating to increase roughness tolerance. Details about the design of this nozzle may be found in Refs. 25 and 26. We note that neither was this nozzle built nor do there exist any current plans to do so.

Figure 18 shows the Mach 2.4 pilot nozzle as well as the associated Mach number contours. As already mentioned, the mean flow computation was done by a two-dimensional/axisymmetric compressible N–S code HTC2D. The conditions considered here are of a stagnation temperature of $T_0 = 80°$R, a stagnation pressure of $P_0 = 200$ psia, and an adiabatic wall condition ($T_w = T_{ad}$). In Fig. 19, we see that the N value of Görtler instability reaches about 9 at the nozzle exit, and the N value of T–S, that is, first-mode, waves only reach a modest value of 4.6. Therefore, as indicated in Ref. 25, at $P_0 = 200$ psia the whole uniform flow test rhombus is expected to be the quiet test core, and as a consequence, the quiet test-core-length Reynolds number $Re_{\Delta x}$ will be expected to reach a value of 80×10^6.

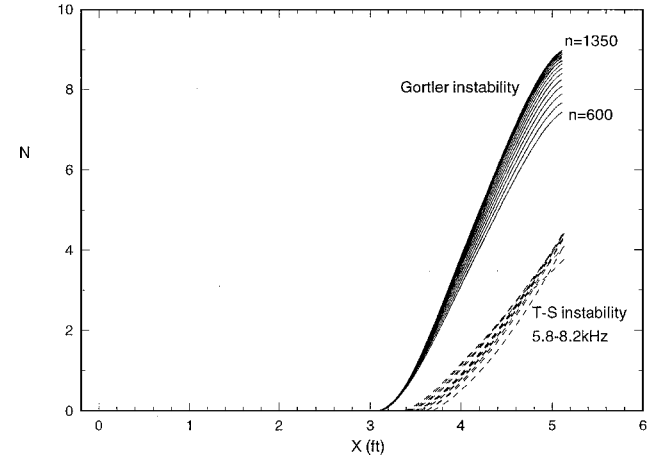

Fig. 19 Computed N values for Görtler vortices with various azimuthal wave numbers n and T–S, that is, first-mode, disturbances in the Mach 2.4 nozzle wall boundary layer for $T_0 = 540°$ R, $P_0 = 200$ psia, and $T_w = T_{ad}$.

For a given unit Reynolds number, in general the surface finish requirements may be relaxed by a factor proportional to the nozzle size. This principle works advantageously toward the Mach 2.4 pilot nozzle, which is relatively large in its size. On the other hand, the increase in unit Reynolds number makes the boundary layer thinner and in turn tightens the surface finish requirement. To determine the surface finish specifications for this nozzle wall, we compute the

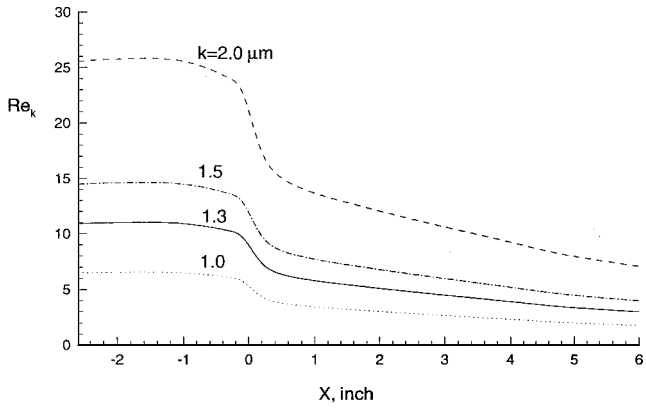

Fig. 20 Distribution of Reynolds number Re_k for various fixed roughness heights, $k = 2.0$, 1.5, 1.3, and 1.0 μm, in Mach 2.4 nozzle for $T_0 = 540°$R, $P_0 = 200$ psia, and $T_w = T_{ad}$ ($Re_{\Delta x} = 80 \times 10^6$).

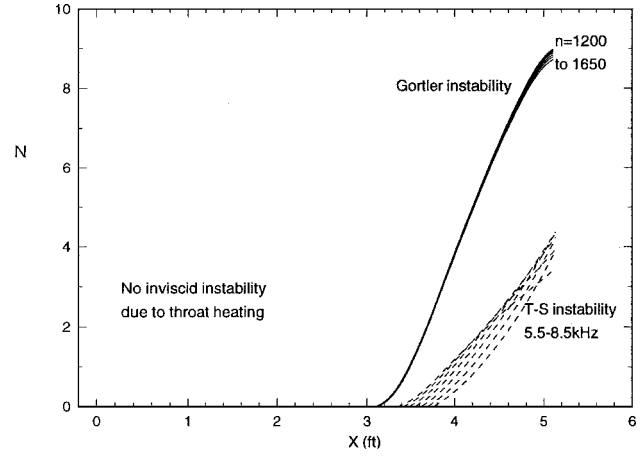

Fig. 21 Computed N values for Görtler vortices and T–S, that is, first-mode, disturbances for $T_0 = 540°$R, $P_0 = 200$ psia, and $T_w = 1.5T_{ad}$ for $x < 5$ in. ($Re_{\Delta x} = 80 \times 10^6$); no inviscid instability.

distribution of roughness Reynolds number Re_k for various fixed roughness heights, that is, $k = 2.0$, 1.5, 1.3, and 1.0 μm, and present results in Fig. 20. With $Re_k = 12$ used as the criterion of allowable surface roughness, results indicate that for an adiabatic wall the surface finish in the critical throat region should meet the requirement of $k < 1.3$ μm. When it is considered that the throat diameter of this nozzle is relatively large, hand polishing can be performed in the throat region. Therefore, it is believed that this roughness height requirement is likely within current manufacturing capability, and as a consequence, throat heating may not be required. However, if heating turns out to be an option, some level of mild heating may suffice.

Because of the large size of this Mach 2.4 nozzle, the limitation imposed by the mass flow requirement may prevent this nozzle from reaching an adiabatic condition. If that happens, the nozzle will be operating in a situation similar to wall cooling resulting in tighter surface finish requirement. Therefore, we consider heating of $T_w = 1.5T_{ad}$ in the region of $x < 5.0$ in. This level of heating raises the wall temperature in the throat region by about 250°R. Figures 21 and 22 show results of stability analyses and Reynolds number Re_k calculations. In this case, no inviscid instability was triggered. It was found that it takes a higher level of heating, for example, $T_w = 2.2T_{ad}$, to bring out the inviscid instability in this nozzle. With $T_w = 1.5T_{ad}$, the critical roughness height could be relaxed from $k < 1.3$ to 2.0 μm. Previous experience with the advanced Mach 3.5 quiet nozzle indicates that a surface finish of $k < 2.0$ μm is within the available manufacturing capability. Hence, with modern manufacturing capability heating at the level of $T_w = 1.5T_{ad}$ should suffice, without triggering the inviscid instability. To summarize, for the Mach 2.4 axisymmetric pilot nozzle, when $Re = 80 \times 10^6$, for adiabatic conditions, $k < 1.3$ μm and for $T_w = 1.5T_{ad}$, $x < 5$ in., $k < 2.0$ μm.

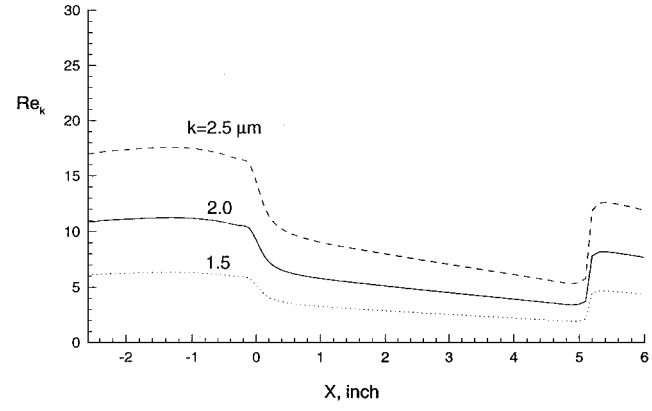

Fig. 22 Distribution of Reynolds number Re_k for various fixed roughness heights, $k = 2.5$, 2.0, and 1.5 μm, for $T_0 = 540°$R, $P_0 = 200$ psia, and $T_w = 1.5T_{ad}$ for $x < 5$ in. ($Re_{\Delta x} = 80 \times 10^6$).

We add a cautionary note. The slow expansion nozzle design concept of Ref. 1 considered only the eigenmodes of the boundary layer and surface quality in the throat region. Small surface irregularities of the nozzle lip could introduce streamwise disturbances that could be amplified downstream in the straight radial flow region of the nozzle. Interaction of freestream vorticity with the nozzle lip could also be a source of streamwise disturbances. At sufficiently high Reynolds numbers, the induced streamwise vortices could breakdown due to secondary instabilities. All such transition scenarios should be carefully evaluated before constructing a quiet high-Reynolds-number national facility.

V. Conclusions

It is found that heating in the throat region in combination with improvements in the surface finish show strong promise in increasing the range of Reynolds number for quiet operation. The present results show that the maximum allowable roughness height for an adiabatic advanced Mach 3.5 axisymmetric quiet nozzle is about $k < 0.75$ μm when the nozzle is operating at its highest design condition. Because of the boundary-layer thickening effect of wall heating, throat heating can be used to relax the surface quality requirements. With a heating level of $T_w = 1.7T_{ad}$, the critical roughness height increases to about $k < 1.7$ μm. In addition, it is found that throat heating has a negligible effect on the Görtler instability. For the Mach 2.4 axisymmetric pilot nozzle, the maximum roughness height can not exceed 1.3 μm for the adiabatic wall condition. Although heating might not be needed, heating of $T_w = 1.5T_{ad}$ can raise the allowable roughness height to $k < 2.0$ μm without associated penalty of triggering inviscid instability.

One effect of throat heating, in combination with the favorable pressure gradient, is to bring out an overshoot in the streamwise velocity profile. Associated with this overshoot is a generalized inflection point near the edge of the boundary layer, which gives rise to a two-dimensional high-frequency inviscid instability. N factors associated with this instability determine the allowable wall heating for transition control.

Note that, in a given design, one must consider favorable (on critical roughness height) as well as adverse (on boundary-layer instability) effects of throat heating. Furthermore, practical aspects of applying heating in the throat area, such as issues regarding actual implementation and the possible effect of induced thermal stresses on surface waviness, must be addressed before the beneficial effect of throat heating on enhancing quiet performance can be realized. In addition, all other possible transition promoters (e.g., streamwise disturbances originating at small surface irregularities of the nozzle lip or due to the interaction of freestream vorticity with the nozzle lip) must be considered before the construction of any high-Reynolds-number quiet facility.

Acknowledgments

This work was supported by NASA under Contract NAS1-20417. Very helpful comments of the reviewers are greatly appreciated.

References

[1]Chen, F.-J., Malik, M. R., and Beckwith, I. E., "Görtler Instability and Supersonic Quiet Nozzle Design," *AIAA Journal*, Vol. 30, No. 8, 1992, pp. 2093, 2094.

[2]Tani, I., "Effect of Two-Dimensional and Isolated Roughness on Laminar Flow," *Boundary Layer and Flow Control*, edited by G. V. Lanchmann, Vol. 2, Pergamon, New York, 1961, pp. 637–656.

[3]von Doenhoff, A. E., and Braslow, A. L., "The Effect of Distributed Surface Roughness on Laminar Flow," *Boundary Layer and Flow Control*, edited by G. V. Lachmann, Vol. 2, 1961, pp. 657–681.

[4]Loftin, L. K., Jr., "Effects of Specific Types of Surface Roughness on Boundary-Layer Transition," NACA Advance Confidential Rept. L5J29a, Feb. 1946.

[5]Schwartzburg, M. A., and Braslow, A. L., "Experimental Study of the Effects of Finite Surface Disturbances and Angle of Attack on the Laminar Boundary Layer of an NACA 64A010 Airfoil with Area Suction," NACA TN 2796, 1952.

[6]Smith, A. M. O., and Clutter, D. W., "The Smallest Height of Roughness Capable of Affecting Boundary-Layer Transition in Low Speed Flow," Douglas Aircraft Co., Rept. ES 26803, 1957.

[7]Gregory, N., and Walker, W. S., "The Effect on Transition of Isolated Surface Excrescences in the Boundary Layer," Aeronautical Research Council, Rept. 13436, 1950.

[8]Klebanoff, P. S., Schubauer, G. B., and Tidstrom, K. D., "Measurements of the Effects of Two-Dimensional and Three-Dimensional Roughness Elements on Boundary-Layer Transition," *Journal of the Aeronautical Sciences*, Vol. 22, No. 11, 1955, p. 803.

[9]Beckwith, I. E., Malik, M. R., and Chen, F.-J., "Nozzle Optimization Study for Quiet Supersonic Wind Tunnels," AIAA Paper 84-1628, June 1984.

[10]Harvey, W. D., Stainback, P. C., Anders, J. B., and Cary, A. M., "Nozzle–Wall Boundary-Layer Transition and Freestream Disturbances and Mach 5," *AIAA Journal*, Vol. 13, No. 3, 1975, pp. 307–314.

[11]Schneider, S. P., "Design of a Mach-6 Quiet-Flow Wind-Tunnel Nozzle Using the *eN* Method for Transition Estimation," AIAA Paper 98-0547, 1998.

[12]Dovgal, A. V., Levchenko, V. Y., and Timofeev, V. A., "Boundary-Layer Control by a Local Heating of the Wall," *Laminar–Turbulent Transition*, edited by D. Arnal and R. Michel Springer-Verlag, Berlin, 1990, pp. 113–121.

[13]Demetriades, A., "Stabilization of a Nozzle Boundary Layer by Local Surface Heating," *AIAA Journal*, Vol. 34, No. 12, 1996, pp. 2490–2495.

[14]Krist, S. L., Biedron, R. L., and Rumsey, C. L., "CFL3D User's Manual (Version 5.0)," NASA TM-1988-208444, Aerodynamics and Acoustics Methods Branch, NASA Langley Research Center, Hampton, VA, June 1998.

[15]Harris, J. E., and Blanchard, D. K., "Computer Program for Solving Laminar, Transitional, or Turbulent Compressible Boundary-Layer Equations for Two-Dimensional and Axisymmetric Flow," NASA TM-83207, Feb. 1982.

[16]Lin, R.-S., Edwards, J. R., Wang, W.-P., and Malik, M. R., "Instabilities of a Mach 2.4 Slow-Expansion Square Nozzle Flow," AIAA Paper 96-0784, Jan. 1996.

[17]Wang, W.-P., Lin, R.-S., and Malik, M. R., "Control of Corner Flow Vortices by Geometry Shaping in Mach 2.4 Rectangular Nozzles," AIAA Paper 97-2228, June 1997.

[18]Chen, F.-J., Malik, M. R., and Beckwith, I. E., "Instabilities and Transition in the Wall Boundary Layers of Low-Disturbance Supersonic Nozzles," AIAA Paper 85-1573, July 1985.

[19]Beckwith, I. E., Chen, F.-J., and Malik, M. R., "Design and Fabrication Requirements for Low-Noise Supersonic/Hypersonic Wind Tunnels," AIAA Paper 88-0143, Jan. 1988.

[20]Malik, M. R., "Numerical Methods for Hypersonic Boundary Layer Stability," *Journal of Computational Physics*, Vol. 86, No. 2, 1990, pp. 376–413.

[21]Spall, R. E., and Malik, M. R., "Goertler Vortices in Supersonic and Hypersonic Boundary Layers," *Physics of Fluids A*, Vol. 1, No. 11, 1989, pp. 1822–1835.

[22]Mack, L. M., "Boundary-Layer Stability Theory," Jet Propulsion Lab. Document 900-277, rev. A., California Inst. of Technology, Pasadena, CA, Nov. 1969.

[23]Mack, L. M., "Linear Stability Theory and the Problem of Supersonic Boundary-Layer Transition," *AIAA Journal*, Vol. 13, No. 3, 1975, p. 278.

[24]Cohen, C. B., and Reshotko, E., "The Compressible Laminar Boundary Layer with Heat Transfer and Arbitrary Pressure Gradient," NACA Rept. 1294, 1956.

[25]Chen, F.-J., and Wilkinson, S. P., "Design of Mach 2.4 Quiet Nozzles for the NASA Langley Supersonic Low-Disturbance Pilot Tunnel," AIAA Paper 94-2506, June 1994.

[26]Wilkinson, S. P., Anders, S. G., Chen, F.-J., and White, J. A., "Status of NASA Langley Quiet Flow Facility Developments," AIAA Paper 94-2498, June 1994.

M. Sichel
Associate Editor